EARLY COVER SPALLING IN HSC BRIDGE PIERS AND AASHTO STRESS BLOCK PARAMETERS

Sungjin Bae, Ph.D. Candidate, Department of Civil Engineering,
The University of Texas at Austin
Oguzhan Bayrak, Assistant Professor of Civil Engineering, Phil M. Ferguson Structural Engineering Laboratory, The University of Texas at Austin

ABSTRACT

In HSC column tests, early spalling of cover concrete has been reported. Although early cover spalling and associated strength loss in HSC columns has been observed by some researchers, a rational way to incorporate this phenomenon in the AASHTO code has not yet been introduced. Moreover, the use of AASHTO stress block parameters to estimate the strength of HSC columns results in unsafe predictions for moment capacity. Based on experimental evidence, it was decided to reduce the ultimate compressive strain limit of AASHTO to 0.0025 for HSC members such that the capacity of these members could be evaluated prior to cover spalling. Two different approaches were proposed and compared: (1) strength modification factor method for the AASHTO stress block parameters, (2) a new set of stress block parameters. Both proposed techniques result in conservative estimations of strength for high-strength concrete column designs as well as normal-strength concrete column designs.

Keywords: bridge piers, cover spalling, high strength concrete, stress block parameters.

INTRODUCTION

When the AASHTO LRFD Bridge Design Specifications[1] were written, there were inadequate data to demonstrate the applicability of the provisions to high-strength concrete (HSC). The FHWA Showcase Projects are encouraging the use of high-performance concrete in bridge structures. High-performance concrete (HPC) used in the construction generally has high strength. This necessitates a careful examination of the use of AASHTO LRFD Bridge Design Specifications[1] for nominal capacity calculations for high-strength concrete (HSC) columns because they are primarily based on the experimental data obtained from normal strength concrete (NSC) column tests.

In HSC column tests, early spalling of cover concrete has been reported by researchers[2,3,4,5]. An extensive literature survey was undertaken to determine the relationship between the cover spalling strain, concrete strength, and the amount and spacing of lateral reinforcement. Only a very limited amount of data on cover spalling strains was found in the literature. Ozden[6] reported that the strains measured at the onset of concrete cover spalling ranged between 0.0026 and 0.0048 for ten HSC column specimens (8 ksi $< f_c' <$ 10 ksi). As part of a comprehensive research program aimed at studying the behavior of HSC columns subjected to axial and flexural loads, Bayrak[5] tested 24 HSC columns (8 ksi $< f_c' <$ 16 ksi). This study showed that in 21 of the 24 columns tested, cover spalling took place at strains smaller than 0.003, the ultimate strain used for column capacity calculations in AASHTO provisions. As experiments show that spalling of concrete cover takes place at strains smaller than 0.003 in HSC columns, it is critical to account for early cover spalling in calculating the capacity of HSC columns.

AASHTO STRESS BLOCK PARAMETERS[1]

The current code provisions for stress block parameters were originally based on the test results from eccentrically loaded unreinforced concrete columns reported by Mattock et al.[7] In their experimental investigation, Mattock et al. employed normal strength concrete ($f_c' <$ 8 ksi). Their work benefited from the previous investigations conducted by Whitney[8] and Hognestad et al.[9]. Nedderman[10] conducted tests on eccentrically loaded unreinforced concrete columns with concrete strengths ranging between 12 and 14 ksi and proposed a lower limit of 0.65 on β_1 for sections with concrete strengths in excess of 8 ksi.

Figure 1 illustrates the rectangular stress block parameters of AASHTO provisions. The intensity of the equivalent stress block is given by $\alpha_1 f_c'$. The depth of the stress block is $\beta_1 c$, where c is the neutral axis depth. According to AASHTO provisions, α_1 is assumed to have a constant value of 0.85. The parameter β_1 is equal to 0.85 for concrete strengths up to 4 ksi and is reduced gradually at a rate of 0.05 for each 1000 psi of concrete strength in excess of 4 ksi to the limit that $\beta_1 \geq 0.65$. The ultimate compressive strain ε_{cu} (Figure 1b) is taken to have a constant value of 0.003 for all concrete strengths.

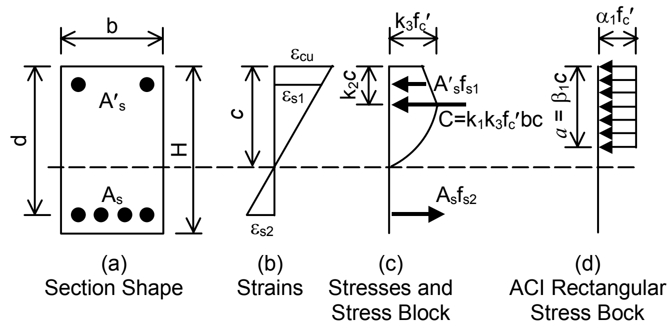

Fig. 1 Rectangular Stress Block

Table 1 summarizes various recommendations for α_1, β_1 and ε_{cu}. The recommendations listed in Table 1 were obtained from the research reported in the literature and various design codes. Although various recommendations made by researchers[11,14,15] and the design codes[1,12,13,16] are considerably different in nature, capacities of reinforced concrete members subjected to low levels of axial load ($P < P_b$) can be predicted with similar levels of accuracy by using any of the aforementioned recommendations. However, for high axial load levels ($P > P_b$), the accuracy of capacity estimations will significantly depend on the accuracy in estimating the position and magnitude of the resultant compressive force of the concrete section. In short, the effect of using accurate and conservative stress block parameters will be pronounced for column sections failing in compression.

Table 1. Rectangular Stress Block Parameters

Reference	α_1	β_1	ε_{cu}
AASHTO[1]	0.85	$1.05-0.05f_c'$ $0.85 \geq \beta_1 \geq 0.65$	0.003
Ibrahim and MacGregor[11]	$0.85-0.009f_c' \geq 0.725$	$0.95-0.017f_c' \geq 0.70$	0.003
CAN 3-A23.3-M94[12]	$0.85-0.009f_c' \geq 0.67$	$0.97-0.017f_c' \geq 0.67$	0.003
NZS3101-1995[13] (or Li et al.[14])	$1.07-0.028f_c'$ $0.85 \geq \alpha_1 \geq 0.75$	$1.05-0.05f_c'$ $0.85 \geq \beta_1 \geq 0.65$	0.003
Azizinamini et al.[15]	$1.35-0.05f_c'$ $0.85 \geq \alpha_1 \geq 0.60$	$1.05-0.05f_c'$ $0.85 \geq \beta_1 \geq 0.65$	0.003
CEB-FIP 1990[16]	$0.85(1-f_c'/36)$	1	$0.004-0.002f_c'/15$

(units: ksi)

LITERATURE ON EARLY COVER SPALLING FOR HSC COLUMNS

The literature survey conducted revealed the fact that early spalling of cover concrete led to lower-than-anticipated failure loads in many experimental investigations[2,3,4,5]. The loss of cover concrete prior to reaching the theoretical load carrying capacity is a peculiar problem that can only be associated with HSC columns. Cusson and Paultre[2] conducted experimental investigations to evaluate the behavior of concentrically loaded HSC columns. They reported that the concrete cover spalled off suddenly, resulting in a 10%~15% drop of axial load. At this point, the confining stresses provided by the transverse reinforcement were activated and the well-confined column specimens displayed a reasonably stable behavior. Results of the experimental investigations conducted by Cusson and Paultre[2] and Razvi and Saatcioglu[17] indicated that in well-confined HSC columns with concrete strengths greater than 11 ksi, the second peak load is approximately equal to, or lower than, the first peak load. When experimental observations reported by researchers[2,3,4,17] are thoroughly examined, it can be concluded that the theoretical capacity of HSC column sections should be based on the early cover spalling event (point A in Figure 2) rather than the ultimate strain of 0.003 (point B in Figure 2). At this point, as the confinement stresses acting on the core concrete are very low, the effect of confinement can be safely neglected. Hence, the strength at the onset of cover spalling can be estimated using an unconfined HSC stress-strain curve.

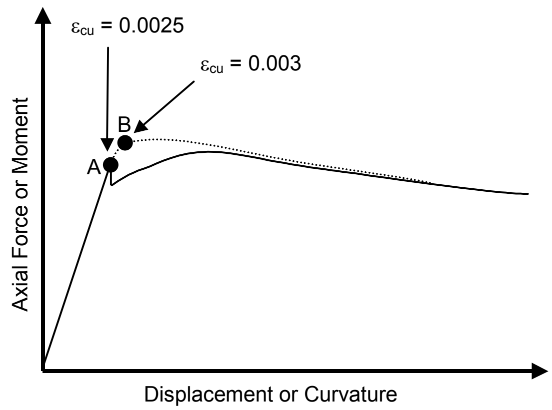

Fig. 2 Effect of Early Cover Spalling on the Response ($P > P_b$)

Early loss of cover concrete happens in most cases for a column with closely spaced ties. There are two factors that contribute to this phenomenon. First, closely spaced ties form a weak plane between the concrete core and the cover which results in an early spalling of concrete cover. Secondly, closely spaced ties result in high confinement efficiency. The stress-strain behavior of the confined core concrete and the unconfined cover concrete can be significantly different, and high shear stresses between the core and the cover concrete may develop and contribute to the early spalling of concrete cover. Foster et al.[3] reported that as the amount of confining reinforcement increased, the cover spalling strains of the HSC specimens tested decreased. Foster[4] also reported that the cover spalling is of concern for HSC columns with high axial loads. Other researchers[2,5] reported that closely spaced ties in HSC columns form a weak plane between the core and the cover concrete resulting in an early spalling of concrete cover.

The majority of the ultimate compressive strains reported in the literature typically range from 0.003 to 0.004 for specimens made using normal strength concrete (2 ksi < f_c' < 8 ksi). As a result, ε_{cu} = 0.003 was adopted by AASHTO provisions. Ibrahim and MacGregor[18] also reported that the maximum concrete compressive strains just prior to cover spalling ranged from 0.0033 to 0.0046 for plain concrete or lightly confined concrete columns made with high strength concrete (9 ksi < f_c' < 19 ksi).

On the other hand, Ozden[6] reported that the cover spalling strains ranged between 0.0026 and 0.0048 for the ten HSC column specimens (8 ksi < f_c' < 10 ksi) tested under eccentric application of axial loads. Bayrak[5] reported that the cover spalling strains ranged between 0.0022 and 0.0032 for the 24 well-confined HSC columns with concrete strengths ranging between 8 ksi and 16 ksi (Figure 3). It is important to note that the presence of lateral reinforcement as specified by the special provisions for seismic design of the AASHTO code would likely lower the cover spalling strains. In fact, this is the main reason why the specimens tested by Bayrak[5] displayed considerably lower cover spalling strains.

Figure 3a shows that the cover spalling strain decreases as the confinement index, $\rho_s \cdot f_{sh}/f_c'$, increases with a considerable amount of scatter. Figure 3b illustrates the lack of correlation between cover spalling strain and concrete strength. Figure 3 clearly demonstrates that the cover spalling strain for HSC columns is lower than the ultimate strain of 0.003 in AASHTO provisions. Considering these, a lower bound on the cover spalling strain of 0.0025 ($\varepsilon_{spalling}$ = 0.0025) is adopted for HSC as the ultimate reliable strain in the research reported herein.

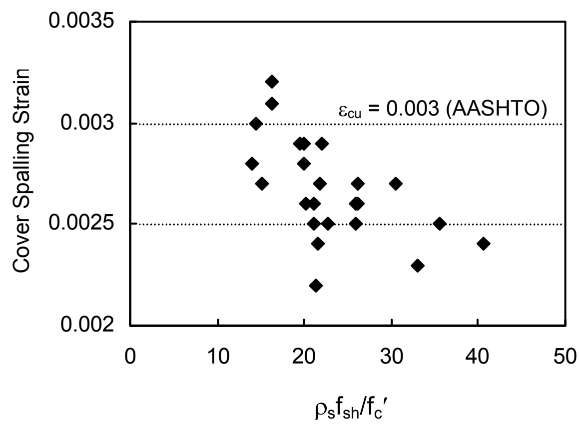

(a) Cover Spalling Strain vs. $\rho_s f_{sh}/f_c'$

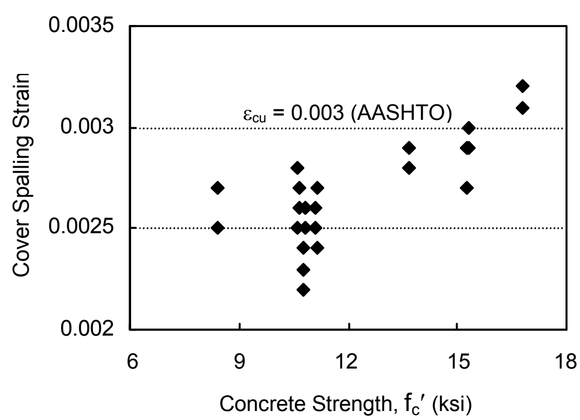

(b) Cover Spalling Strain vs. Concrete Strength

Fig. 3 Cover Spalling Strains of HSC Columns

CONCRETE MODEL

The stress-strain response of unconfined HSC was modeled using the suggestion of Popovics[19]. Tomaszewicz[20] and Thornfeldt et al.[21] proposed Equation 1 based on the equations recommended by Popovics[19], and then Collins et al.[22] modified some of the parameters to obtain this equation. This model is applicable to a wide range of concrete strengths. For concrete strengths up to 16 ksi, this model offered a very good approximation of the experimentally measured behavior of HSC cylinders tested by Bayrak[5]. Equations 1 through 5 summarize the stress-strain relationship proposed by Collins et al.[22]

$$\sigma_c = f_c' \frac{\varepsilon_c}{\varepsilon_c'} \frac{n}{n-1+(\varepsilon_c/\varepsilon_c')^{nk}} \tag{1}$$

where,

$$\varepsilon_c' = \frac{f_c'}{E_c}\frac{n}{n-1} \tag{2}$$

$$n = 0.8 + \frac{f_c'}{2500} \tag{3}$$

$$k = 0.67 + \frac{f_c'}{9000} \qquad (\ k = 1 \text{ for } \varepsilon_c/\varepsilon_c' \le 1\ ) \tag{4}$$

$$E_c = 40{,}000\sqrt{f_c'} + 1{,}000{,}000 \tag{5}$$

Note that in Equations 1 through 5, f_c' is expressed in terms of psi. Equation 5 was proposed by Carrasquillo et al.[23]

STRENGTH MODIFICATION FACTORS

The premature cover spalling in HSC columns results in the reduction of strength (Figure 2). As mentioned earlier, a lower bound value of 0.0025 is adopted as the cover spalling strain in HSC columns. To account for the reduction of axial force or flexural moment strength due to premature cover spalling, two strength modification parameters are introduced as follows:

ξ_1 = axial force reduction parameter due to premature cover spalling

$$= \frac{P_{2.5}}{P} \tag{6}$$

ξ_2 = moment reduction parameter due to premature cover spalling

$$= \frac{M_{2.5}}{M} \tag{7}$$

where,

$P_{2.5}$ = maximum axial strength up to $\varepsilon_{spalling}$ = 0.0025 (Figure 2)
$M_{2.5}$ = maximum moment strength up to $\varepsilon_{spalling}$ = 0.0025 (Figure 2)
P = maximum axial load carrying capacity without considering premature cover spalling in the analysis (Figure 2)

M = maximum moment capacity without considering premature cover spalling in the analysis (Figure 2)

$P_{2.5}$, $M_{2.5}$, P, and M are calculated using a sectional analysis program developed during the course of this research. The cover concrete of a section is assumed to follow the stress-strain curve for the gross cross section before spalling of the cover concrete at the spalling strain of 0.0025. When the uppermost compressive concrete cover fiber reaches the spalling strain, the load-carrying capacity of the entire top compressive concrete cover is taken to be equal to zero in the analyses. This is consistent with the experimental observations where spalling of the concrete cover as a whole was observed in all the 24 tests conducted by Bayrak[5].

Parametric studies have been conducted to evaluate the influence of cover thickness, section size, amount and distribution of longitudinal reinforcement, concrete strength, and level of axial force on ξ_1 and ξ_2. Square column sections (20″×20″ and 30″×30″) with a cover thickness "t" have been considered in the parametric studies.

THE EFFECT OF COVER THICKNESS

At very small cover thickness, ξ_1 and ξ_2 tend to decrease as the cover thickness increases (Figures 4 and 5). However, within the practical range of cover thickness (t/H=0.05~0.15), ξ_1 and ξ_2 are almost constant. This is similar to the conclusions reported by Liu et al.[24] It is important to note that both ξ_1 and ξ_2 decrease with increasing concrete strength. In other words, premature cover spalling and capacity loss associated with it becomes more pronounced as concrete strength increases.

THE EFFECT OF SECTION SIZE

In order to investigate the influence of section size on ξ_1 and ξ_2, 20″×20″ and 30″×30″ square sections were utilized in the parametric studies. Various cover thickness, longitudinal reinforcement ratio, and axial load levels were employed in the parametric studies conducted. Figure 6 illustrates the results from parametric studies where the ratio of cover thickness to overall section height, longitudinal reinforcement ratio, and axial force were taken as 0.1, 1.0%, $0.5P_o$, respectively. An examination of Figure 6 indicates that the section size had no influence on ξ_1 and ξ_2. The validity of this observation was verified for the entire spectrum of concrete strengths, but some of the results are not presented here due to space limitations.

THE EFFECT OF AMOUNT OF LONGITUDINAL REINFORCEMENT

Figure 7 illustrates the analyses results where ξ_1 and ξ_2 were calculated for two different longitudinal reinforcement ratios of 1.0% and 8.0%, which are the lower and upper limits used in AASHTO provisions. The cases presented in Figure 7 are those in which the ratio of cover thickness to overall section height and axial force were 0.1 and $0.5P_o$, respectively. The influence of the amount of longitudinal reinforcement on ξ_1 and ξ_2 were more pronounced for higher concrete strengths. For sections where concrete strength was 17 ksi, an increase in the amount of longitudinal reinforcement ratio from 1% to 8% resulted in an increase of ξ_1 from 0.87 to 0.89 for the practical range of cover thickness. For the case considered above, ξ_2 increased from 0.73 to 0.76. It is important to note that these are small changes relative to the magnitude of ξ_1 and ξ_2.

THE EFFECT OF DISTRIBUTION OF LONGITUDINAL REINFORCEMENT

Figure 8 shows the results from parametric studies where two different longitudinal reinforcement distribution cases were considered. In case 1, longitudinal reinforcement was placed at the tension and compression faces of a column sections. In case 2, longitudinal reinforcement was distributed uniformly along the four sides of a column section. Various amounts of longitudinal reinforcement were considered in the parametric studies conducted. However, Figure 8 illustrates results from the analyses where a longitudinal reinforcement ratio was equal to 1%. As can be observed in this figure, the effect of the distribution of longitudinal reinforcement on ξ_2 is negligible for all practical purposes.

STRENGTH REDUCTION PARAMETERS: ξ_1 AND ξ_2

From the parametric studies conducted, it is concluded that the strength reduction parameters are not influenced by cover thickness or section size. However, they are greatly influenced by concrete strength and the level of axial load. As ξ_1 and ξ_2 are insignificantly influenced by the amount and distribution of longitudinal reinforcement, the amount and distribution of longitudinal reinforcement in the expressions ξ_1 and ξ_2 expressions are not included.

Figure 9 shows the relationships between ξ_1 and ξ_2 and concrete strength. As can be seen in Figure 9, the concrete strength is the primary factor that affects the axial force reduction parameter due to premature cover spalling, ξ_1. The moment reduction parameter due to premature cover spalling, ξ_2, is a function of concrete strength and axial force. As concrete strength increases, both ξ_1 and ξ_2 decrease. An increase in the level of axial load results in considerable reductions in ξ_2. Figure 9 illustrates both the analytical results (solid lines) and the simplified equations adopted (Equations (8) and (9)).

$$\begin{aligned} \xi_1 &= 1 - \frac{1}{43.5}\left(f'_c - 11\right) && \text{for } f'_c \geq 11 \text{ ksi} \\ &= 1 && \text{for } f'_c < 11 \text{ ksi} \end{aligned} \tag{8}$$

$$\begin{aligned} \xi_2 &= 1 - \frac{1}{15.4}\left(\frac{P^*}{P_0}\right)\left(f'_c - 8\right) \\ &= 1 - \frac{1}{15.4}\xi_1\left(\frac{P}{P_0}\right)\left(f'_c - 8\right) && \text{for } f'_c \geq 8 \text{ ksi} \\ &= 1 && \text{for } f'_c < 8 \text{ ksi} \end{aligned} \tag{9}$$

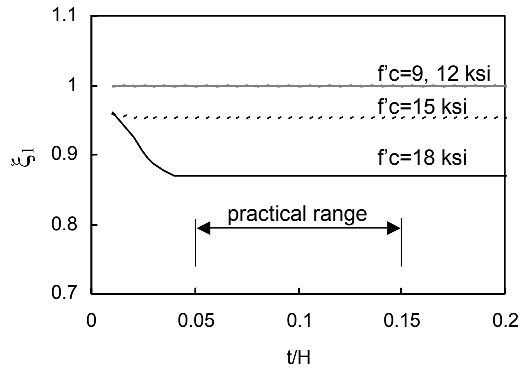

Fig. 4 Relationship between ξ_1 and Cover Thickness (t/H)

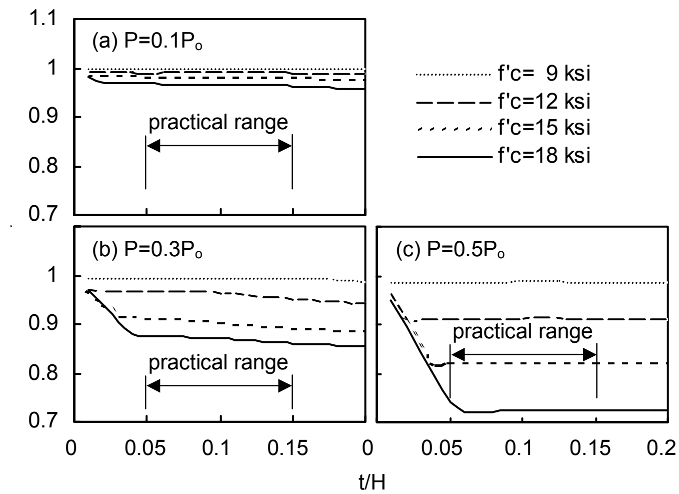

Fig. 5 Relationship between ξ_2 and Cover Thickness (t/H)

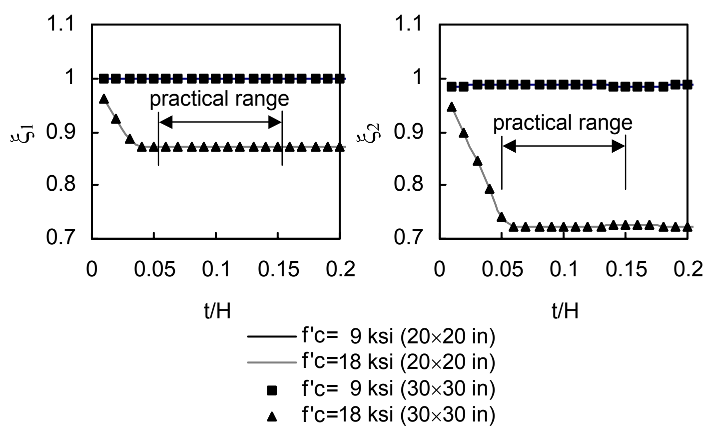

Fig. 6 Relationship between ξ_1, ξ_2 and Section Size

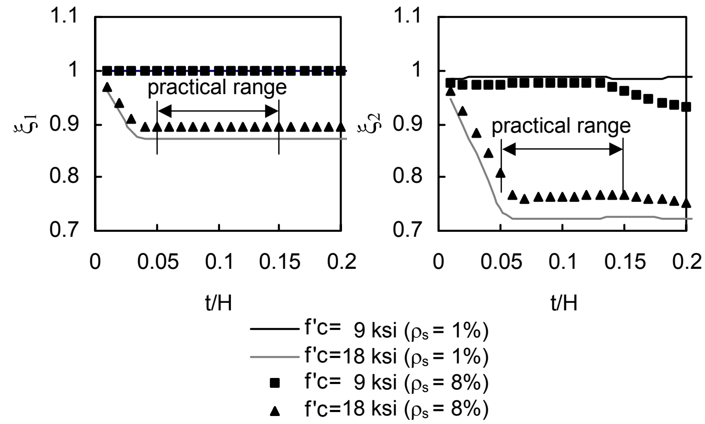

Fig. 7 Relationship between ξ_1, ξ_2 and Amount of Reinforcement

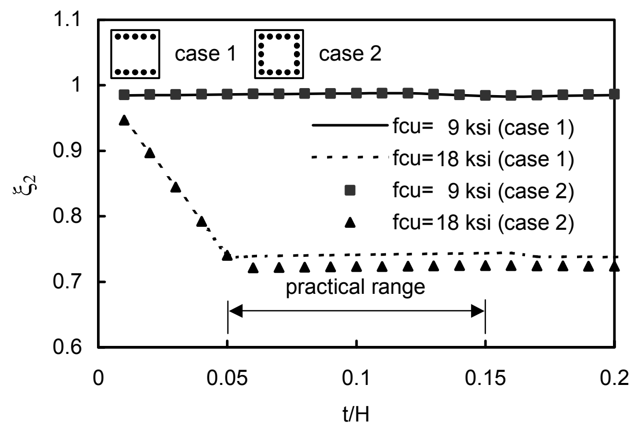

Fig. 8 Relationship between ξ_2 and Distribution of Reinforcement

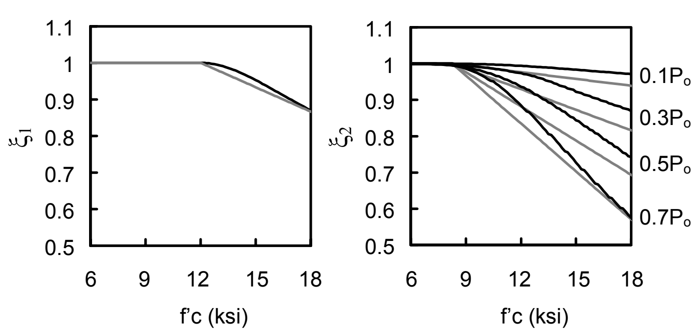

Fig. 9 Relationship between ξ_1, ξ_2 and Concrete Strength

The axial force, P, and bending moment, M, calculated using AASHTO provisions can be modified to obtain the reduced axial force, P^*, and bending moment, M^* values (Equations (10) and (11)).

$$P^* = \xi_1 \times P \tag{10}$$
$$M^* = \xi_2 \times M \tag{11}$$

A NEW SET OF STRESS BLOCK PARAMETERS

The first step in deriving stress block parameters is to find the position of the resultant force. The position of the resultant force, which is the location of the centroid of the shaded area, is represented by the parameter $\beta_1 \cdot c/2$. The parameter α_1 is then determined by equating the area under the actual stress-strain curve to the area under the rectangular stress block (Figure 1). Equations 12 and 13 illustrate the analytically derived expressions for α_1 and β_1. In deriving the stress block parameters, the maximum reliable strain is assumed as the assumed cover spalling strain of 0.0025. It is important to note that these equations have no practical significance and hence they are simplified later in this section.

$$\alpha_1 = 5.2\times10^{-6}\left(f'_c\right)^4 - 1.8\times10^{-4}\left(f'_c\right)^3 + 1.0\times10^{-4}\left(f'_c\right)^2 - 6.5\times10^{-3}\left(f'\right)_c + 0.9607 \tag{12}$$
$$\beta_1 = -2.9\times10^{-6}\left(f'_c\right)^4 + 1.1\times10^{-4}\left(f'_c\right)^3 - 4.6\times10^{-4}\left(f'_c\right)^2 - 2.3\times10^{-2}\left(f'_c\right) + 0.8812 \tag{13}$$

Figure 10a shows the analytically derived curve for β_1 (Equation 13) and the experimental data. The analytically derived β_1 and AASHTO (or NZS) expressions establish a lower bound to the experimental data. The CAN A23.3-94 (CAN) expression for β_1 passes through the center of the data. Figure 10b presents a comparison between various expressions for α_1 and experimental data. As can be seen in this figure the analytically derived α_1 passes through the center of the data up to a concrete strength of about 15 ksi and falls below the data beyond this concrete strength. The CAN expression for α_1 establishes a lower bound to the experimental data.

It is interesting to note that the general trend of parameters α_1 and β_1 of the analytically derived expressions and the Canadian code are somewhat contradictory, in that when one approach results in a line that passes through the center of the data that the other traces a lower bound to the data and vice versa. This is because the Canadian code equations were determined to provide a conservative estimate for the column capacity, while the analytically derived parameters are determined directly from the stress-strain curve. The $\alpha_1\beta_1$ term obtained through the use of Equations 12 and 13 and the Canadian code are, however, very similar (Figure 10c). Both analytically derived $\alpha_1\beta_1$ and CAN equations give a lower bound estimation of resultant forces. AASHTO equations give higher compressive forces than the experimental data starting at a concrete strength of about 11 ksi. Meanwhile, the use of a different α_1 expression in the New Zealand code[13] also gives lower (i.e. conservative) compressive forces (Figure 10c).

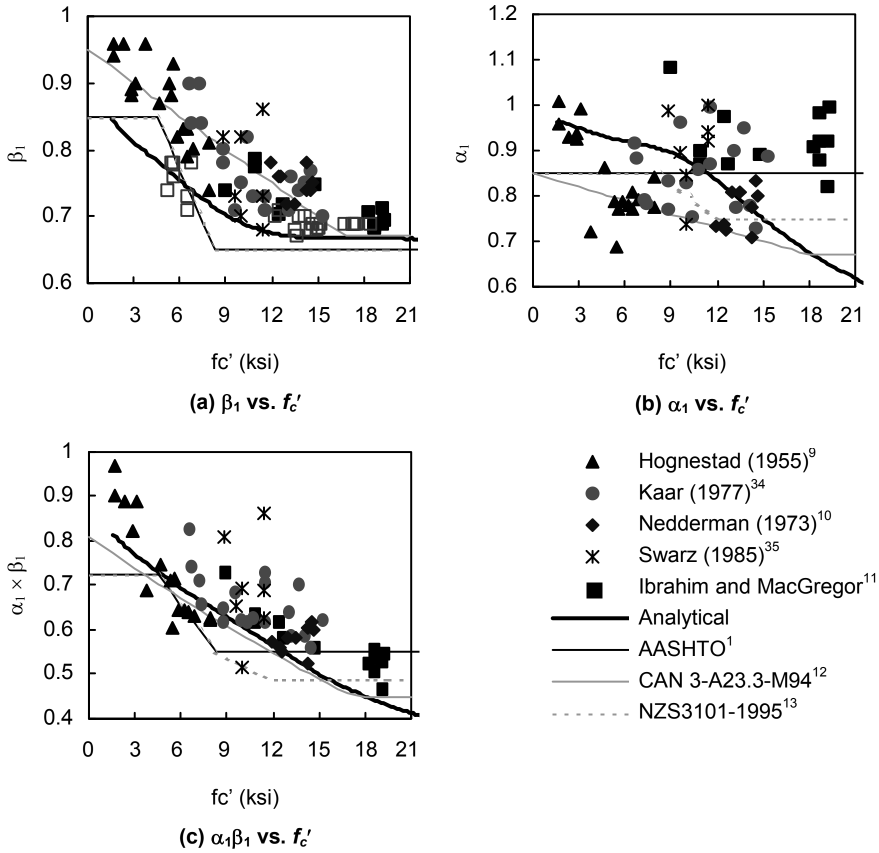

Fig. 10 Concrete Stress Block Parameters α_1 and β_1: Experiments vs. Various Models

In order to be consistent with the current AASHTO expressions for normal strength concrete (and considering the fact that the β_1 expression in AASHTO shows a similar trend to the expression proposed herein), the following concrete stress block parameters are proposed:

$\alpha_1 = 1.13 - 0.28 f_c'$ where $0.67 \leq \alpha_1 \leq 0.85$ (f_c' in ksi) (14)

$\beta_1 = 0.97 - 0.28 f_c'$ where $0.67 \leq \alpha_1 \leq 0.85$ (f_c' in ksi) (15)

$\varepsilon_{cu} = 0.0025$ for f_c' greater than 8 ksi, otherwise $\varepsilon_{cu} = 0.003$

The lower bound value for β_1 is established based on the analytically calculated value as shown in Figure 10a and the one for α_1 is established using a triangular stress-strain curve. The shape of the actual stress-strain curve for concrete with $f_c' \geq 15$ ksi is similar to a triangular stress distribution. If the maximum stress of the triangular stress distribution in HSC is assumed to be 0.9 f_c' at the cover spalling strain of 0.0025, the stress block parameters $\alpha_1\beta_1$ and $\beta_1/2$ can be calculated as 0.45 and 0.33, respectively. The use of the proposed expressions (Equations 14 and 15) yields 0.45 and 0.34 for $\alpha_1\beta_1$ and $\beta_1/2$, respectively.

CORROBORATION WITH EXPERIMENTAL DATA

The accuracy and conservativeness of the proposed stress block parameters are evaluated using data from 224 column tests reported in the literature[5,6,9,15,18,25-33]. All of the 224 columns had reasonably large rectangular sections. Of the 224 columns, Bayrak[4] tested 24 columns in order to study the behavior of HSC columns as part of the ongoing research program. The columns had various amounts of lateral reinforcement ranging from lightly-confined columns to well-confined concrete columns containing more reinforcement than that required by AASHTO provisions. As this research focuses on the moment capacity predictions obtained through the use of various stress block parameters, data on eccentrically loaded columns and columns subjected to axial and flexural loads are considered herein.

ERROR MEASUREMENTS

The degree of accuracy of the proposed method can be expressed in two different ways:

1. Error based on the experimental eccentricity is the distance between predicted and experimental strength points (measured on a straight line connecting the origin and the predicted and experimental strength points) divided by the distance between the origin and the experimental strength point on the interaction diagram.

$$E_e = \frac{\sqrt{(M_{pre,1}/M_o)^2 + (P_{pre,1}/P_o)^2} - \sqrt{(M_{exp}/M_o)^2 + (P_{exp}/P_o)^2}}{\sqrt{(M_{exp}/M_o)^2 + (P_{exp}/P_o)^2}} \times 100 \ (\%) \tag{16}$$

2. Error based on the experimental axial force is the ratio of the difference between the predicted and experimental moment capacities to experimental moment capacity.

$$E_p = \frac{M_{pre,2} - M_{exp}}{M_{exp}} \times 100 \ (\%) \tag{17}$$

where

M_{pre}, P_{pre} = predicted values by the code or proposed method

M_{exp}, P_{exp} = experimental values

M_o, P_o = pure flexural or axial capacity based on AASHTO provisions

The negative sign in error measurements means predicted capacities are less than experimental capacities and hence the prediction is conservative.

RESULTS AND DISCUSSION

The capacities of the 224 columns were estimated by using AASHTO LRFD Specifications [5], CAN A23.3-94[7], NZS3101:95[8], stress block parameters proposed by Ibrahim and MacGregor[14], Azizinamini et al.[16], and the proposed equations. The estimations were

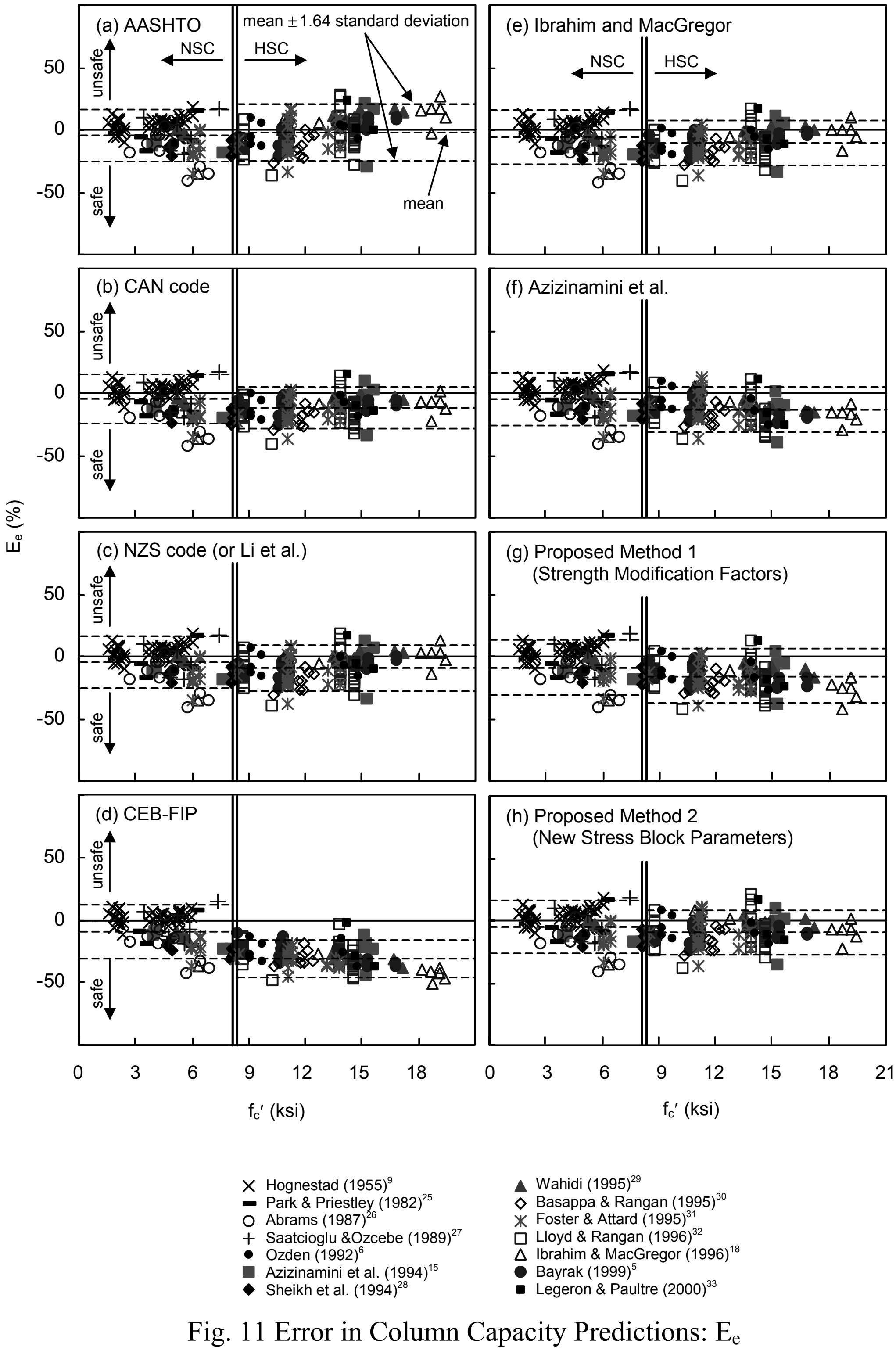

Fig. 11 Error in Column Capacity Predictions: E_e

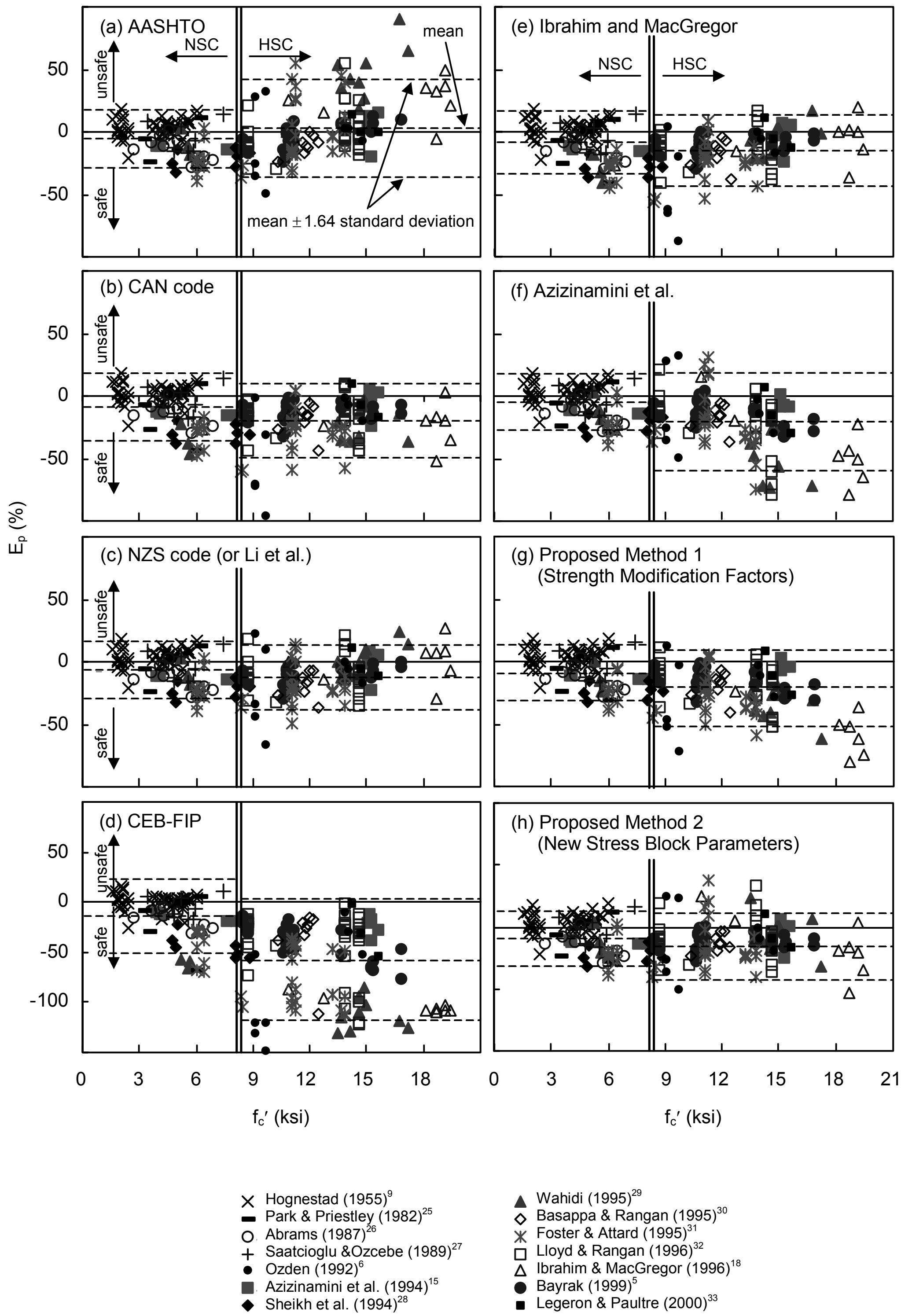

Fig. 12 Error in Column Capacity Predictions: E_p

compared with the test results. Figures 11 and 12 show the accuracy of nominal capacity estimations. For normal statistical distribution, 90% of the data would fall in the range of mean +1.64 × (standard deviation) and mean -1.64 × (standard deviation) by definition. As can be seen in Figures 11 and 12, mean values and +/-1.64 × (standard deviations) are calculated for NSC and HSC such that accuracy can be evaluated for NSC and HSC separately.

The predictions based on eccentricity have been used to evaluate the accuracy of various stress block parameters. Figure 11 illustrates the errors in predictions based on this traditional method. It is interesting to note that there are not significant differences between the results obtained from the use of various stress block parameters. The use of AASHTO stress block parameters yield unsafe estimations for column capacity as concrete strength increases. However, the magnitudes of the unsafe estimations are not unreasonably large. The CEB-FIP stress block parameters are less accurate and too conservative for HSC. The accuracy of all other stress block parameters appear to be reasonably similar based on Figure 11. Proposed two methods show similar trends except some differences at very high concrete strengths ($f_c' > 18$ ksi). At this range of concrete strength, the strength estimations are governed by lower bound limit values.

Columns under earthquake type loads would be subjected to increasing bending moments and shear forces under roughly constant axial loads. In such circumstances, the accuracy of moment capacity predictions becomes an important design issue. Hence, the error measurements based on constant axial load is also employed herein. Figure 12 illustrates that the error measurements based on constant axial force are more sensitive than those based on constant eccentricity (Figure 11). An examination of Figure 12 indicates that the use of AASHTO stress block parameters results in inaccurate and progressively increasing overestimations of the moment capacities as the concrete strength increases. The use of CSA A23.3-94, NZS 3101:95 stress block parameters and those proposed by Ibrahim and MacGregor provide more accurate estimations, but CSA A23.3-94 is generally more conservative. The levels of accuracy and conservativeness of proposed methods are very similar for the entire range of concrete strength. However, it is observed that the proposed stress block parameters yield better estimations. The stress block parameters proposed by Ibrahim and MacGregor and Li et al. also show good levels of accuracy and conservativeness. Figure 12 also shows that the use of CEB-FIP provisions and the stress block parameters recommended by Azizinamini et al. result in inaccurate and progressively increasing underestimations of strength as concrete strength increases. It is believed that design guidelines should provide similar levels of conservativeness for NSC as well as HSC. In this regard, it can be stated that the current AASHTO stress block parameters may not be suitable for use in designing members subject to flexural and axial loads for HSC.

NZS 3101:1995 and CAN A23.3-94 stress block parameters are equally successful in predicting the strength of 224 columns considered in this study. It is interesting to note that the foundation of the proposed expressions and those presented in NZS 3101:1995 and CAN A23.3-94 are significantly different but the impact of such fundamental differences in the end result (i.e. the accuracy and conservativeness of the expressions) appears to be insignificant.

Table 2(a). Mean, Standard Deviation, and Coefficient of Variation in E_e

Reference	NSC ($f_c' < 8$ ksi)			HSC ($f_c' \geq 8$ ksi)		
	Mean	Standard Deviation	Coefficient of Variation	Mean	Standard Deviation	Coefficient of Variation
AASHTO	-4.5*	12.6	-2.8	-1.9	13.3	-6.9
CAN	-6.2	12.7	-2.1	-12.0	9.8	-0.8
NZS	-4.4	12.6	-2.9	-9.0	11.1	-1.2
CEB-FIP	-8.0	12.9	-1.6	-29.2	8.7	-0.3
Ibrahim and MacGregor	-5.9	12.7	-2.1	-10.0	10.4	-1.0
Azizinamini	-4.5	12.6	-2.8	-13.0	10.5	-0.8
Proposed Method 1	-6.2	12.2	-2.0	-10.2	12.4	-1.2
Proposed Method 2	-4.2	12.5	-3.0	-9.1	10.8	-1.2

Table 2(b). Mean, Standard Deviation, and Coefficient of Variation in E_p

Reference	NSC ($f_c' < 8$ ksi)			HSC ($f_c' \geq 8$ ksi)		
	Mean	Standard Deviation	Coefficient of Variation	Mean	Standard Deviation	Coefficient of Variation
AASHTO	-5.3	13.4	-2.5	3.2**	23.3	7.2
CAN	-8.8	16.1	-1.8	-19.3	17.4	-0.9
NZS	-5.2	13.5	-2.6	-10.8	15.3	-1.4
CEB-FIP	-13.3	21.4	-1.6	-58.4	37.7	-0.6
Ibrahim and MacGregor	-8.2	15.5	-1.9	-14.4	16.6	-1.2
Azizinamini	-5.3	13.4	-2.5	-20.9	23.3	-1.1
Proposed Method 1	-7.5	13.7	-1.8	-11.1	15.6	-1.4
Proposed Method 2	-5.1	13.5	-2.6	-10.8	15.9	-1.5

(unit: percentage)

* : negative sign = safe prediction
**: positive sign = unsafe prediction

Table 2 shows the mean, standard deviation, and coefficient of variation values of various proposals for NSC and HSC. This table clearly illustrates that AASHTO stress block parameters produce reasonable estimations for NSC but their use for HSC results in overestimated moment capacities in HSC and increased scatter. The stress block parameters of CEB-FIP and those proposed by Azizinamini tend to yield very conservative estimations, and eliminate the advantages of using HSC. The stress block parameters of CAN, NZS, and Ibrahim and MacGregor give similar levels of accuracy and scatter. The two methods proposed here also result in reasonably good levels accuracy, but the new stress block parameters (Proposed Method 2) are somewhat more accurate.

CONCLUSIONS

- For the 224 columns considered in this study, the use of AASHTO stress block parameters resulted in progressively increasing overestimations of moment capacities as the concrete strength increased. The fact that the unsafe nature of the AASHTO provisions for stress block parameters is systematic suggests that a physical phenomenon that does not affect NSC column capacities does affect HSC column capacities. This phenomenon is believed to be the early cover spalling in HSC columns.

- Having recognized the early cover spalling problem for HSC columns, two different approaches are studied: (1) Strength reduction factors, (2) Stress block parameters.

  1. Strength reduction factors, ξ_1 and ξ_2, were derived analytically and simplified in order to be adopted by practicing engineers with ease. The validity of the strength reduction parameters, i.e. the use of ξ_1 and ξ_2, was evaluated using experimental data from 224 column tests. Parametric sensitivity studies were conducted to identify significant variables to be included in the expressions for ξ_1 and ξ_2. It was found that the cover thickness, section size, and the amount and distribution of longitudinal reinforcement do not influence ξ_1 and ξ_2. The concrete strength and the level of axial load are the only variables that influence ξ_1 and ξ_2 significantly. Based on this observation, simple equations were derived for the strength reduction parameters. Combining these with the current AASHTO provisions, the proposed procedure incorporates the effects of early cover spalling in HSC columns in capacity calculations.

  2. New stress block parameters, α_1 and β_1, are proposed based on the research reported herein. The proposed parameters are as follows:

     $$\alpha_1 = 1.13 - 0.28 f_c' \quad \text{where } 0.67 \le \alpha_1 \le 0.85 \quad (f_c' \text{ in ksi})$$
     $$\beta_1 = 0.97 - 0.28 f_c' \quad \text{where } 0.67 \le \alpha_1 \le 0.85 \quad (f_c' \text{ in ksi})$$

     It is important to note that the proposed stress block parameters are based on the analyses in which $\varepsilon_{cu} = 0.0025$ was employed for maximum useful compressive strain in concrete prior to early cover spalling in HSC ($f_c' \ge 8$ ksi). For NSC the current AASHTO value of $\varepsilon_{cu} = 0.003$ was used. Although the stress block parameters used here are derived using two distinct ultimate strain values, i.e. $\varepsilon_{cu} = 0.003$ for NSC and $\varepsilon_{cu} = 0.0025$ for HSC, the proposed stress block parameters provide a smooth transition from NSC to HSC. In fact, only one set of stress block parameters applicable to the entire range of concrete strength has been proposed herein.

- Proposed methods do provide similar levels of accuracy and conservativeness for NSC and HSC. Stress block parameters proposed by Li et al. and Ibrahim and Macgregor showed similar predictions for section capacities.

REFERENCES

1. The American Association of State Highway and Transportation Officials (1998). "*AASHTO LRFD Bridge Design Specifications, Second Edition*," Washington, D.C.
2. Cusson, D. and Paultre, P. (1994). "High-Strength Concrete Columns Confined By Rectangular Ties," *Journal of Structural Engineering*, 120(3), 783-804.
3. Foster, S.J., Liu, J., Sheikh, S. (1998). "Cover Spalling in HSC Columns Loaded in Concentric Compression," *Journal of Structural Engineering*, 124(12), 1431-1437.
4. Foster, S.J. (2001). "On Behavior of High-Strength Concrete Columns: Cover Spalling, Steel Fibers, and Ductility," *ACI Structural Journal*, 98(4), 583-589.
5. Bayrak, O. (1999). "Seismic Performance of Rectilinearly Confined High Strength Concrete Columns," PhD dissertation, University of Toronto, pp. 80-187.
6. Ozden, S. (1992). "Behavior of High-Strength Concrete Under Strain Gradient," Master's Thesis, University of Toronto, Toronto, Ontario, Canada, 112-113.
7. Mattock, A.H., Kriz, L.B., and Hognestad, E. (1961). "Rectangular Concrete Stress Distribution in Ultimate Strength Design," *Journal of The American Concrete Institute*, 57(8), 875-928.
8. Whitney, C.S. (1937). "Design of Reinforced Concrete Members Under Flexure and Combined Flexure and Direct Compression," *Journal of The American Concrete Institute*, 33(4), 483-498.
9. Hognestad, E., Hanson, N.W., and McHenry, D. (1955). "Concrete Stress Distribution in Ultimate Strength Design," *Journal of the American Concrete Institute*, 52(28), 455-479.
10. Nedderman, H. (1973) "Flexural Stress Distribution in Very High Strength Concrete," M.A.Sc. Thesis, Department of Civil Engineering, University of Texas, Arlington, Texas.
11. Ibrahim, H.H.H. and MacGregor, J.G. (1997). "Modification of the ACI Rectangular Stress Block for High-Strength Concrete," *ACI Structural Journal*, 94(1), 40-48.
12. Canadian Standards Association (1994). "Design of Concrete Structures in Buildings," (*CAN 3-A23.3-M94*), Rexdale, Ontario, Canada.
13. Standards New Zealand (1995), "Design of Concrete Structure," (*NZS 3101-1995*), Wellington, New Zealand.
14. Li Bing, Park, R. and Tanaka, H. (1994). "Strength and Ductility of Reinforced Concrete Members and Frames Constructed using High-Strength Concrete," Research Report No. 94-5, Department of Civil Engineering, University of Canterbury, Christchurch, New Zealand, 373.
15. Azizinamini, A., Kuska, S.B., Brungardt, P., and Hatfield, E. (1994). "Seismic Behavior of Square High-Strength Concrete Columns," *ACI Structural Journal*, 91(3), 336-345.
16. CEB-FIP Model Code 1990 (1990), *Comite Euro-International du Beton*, Thomas Telford, pp.33-42 and 148-149.
17. Razvi, S.R., and Saatcioglu, M. (1996). "Tests of High-Strength Concrete Columns under Concentric Loading," Report OCEERC 96-03, University of Ottawa, Canada.
18. Ibrahim, H.H.H. and MacGregor, J.G. (1996). "Tests of Eccentrically Loaded High-Strength Concrete Columns," *ACI Structural Journal*, 93(5), 585-594.
19. Popovics, S. (1973). "A Numerical Approach to the Complete Stress-Strain Curve of Concrete, Cement and Concrete Research," Pergamon Press Inc., Vol. 3, 583-599.

20. Tomaszewicz, A. (1984). "Stress-Strain Relationship for Concrete," Report No. STF65A84065, Cement and Concrete Institute (SINTEF div. FCB), Trondheim-NTH.
21. Thornfeldt, E., Tomaszewicz, A., and Jensen, J.J. (1987). "Mechanical Properties of High-Strength Concrete and Applications in Design," *Proc., Utilization of High Strength Concrete*, Stavanger, Norway, Tapir, Trondheim, 149-159.
22. Collins, M.O., Mitchell, D., and MacGregor, J.G. (1993). "Structural Design Considerations for High-Strength Concrete," *Concrete International*, 15(5), 27-34.
23. Carrasquillo, R.L., Nilson, A.H., and Slate, F.O. (1981). "Properties of High-Strength Concrete Subject to Short-Term Loads," *Journal of the American Concrete Institute*, Farmington Hills, Michigan, 78(3), 171-178.
24. Liu, J., Foster, S.J., Attard, M.M. (2000). "Strength of Tied High-Strength Concrete Columns Loaded in Concentric Compression," *ACI Structural Journal*, 97(1), 149-156.
25. Park, R. and Priestley, M.J.N. (1982). "Ductility of Square-Confined Concrete Columns," *Journal of the Structural Division*, ASCE, 108(4), 929-950.
26. Abrams, D. (1987). "Influence of Axial Force Variations on Flexural Behavior of Reinforced Concrete Columns," *ACI Structural Journal*, 84(3), 246-254.
27. Saatcioglu, M. and Ozcebe, G. (1989). "Response of Reinforced Concrete Columns to Simulated Seismic Loading," *ACI Structural Journal*, 86(1), 3-12.
28. Sheikh, S.A., Shah, D.V., and Khoury, S.S. (1994). "Confinement of High-Strength Concrete Columns," *ACI Structural Journal*, 91(1), 100-111.
29. Wahidi, S.A.A. (1995). "Strength and Behavior of Reinforced Concrete Columns Made from High Performance Materials," PhD dissertation, University of Texas at Austin, Austin, Texas.
30. Basappa, R.H. and Rangan, B.V. (1995). "Strength of High Strength Concrete Columns under Eccentric Compression," Research Report No 2/95, School of Civil Engineering, Curtin University of Technology, pp. 12-25.
31. Foster, S.J. and Attard, M.M. (1997). "Experimental Tests on Eccentrically Loaded High-Strength Concrete Columns", *Journal of the American Concrete Institute*, 94(3), 295-303.
32. Lloyd, N.A. and Rangan B.V. (1996). "Studies on High-Strength Concrete Columns under Eccentric Compression," *ACI Structural Journal*, 93(6), 631-638.
33. Legergon, F. and Paultre, P. (2000). "Behavior of High-Strength Concrete Columns under Cyclic Flexure and Constant Axial Load," *ACI Structural Journal*, 97(4), 591-601.
34. Kaar, P.H., Hanson, N.W., and Capell, H.T. (1977). "Stress-Strain Characteristics of High-Strength Concrete," *Research and Development Bulletin RD051.01D*, Portland Cement Association, Skokie, Illinois.
35. Swartz, S.E., Nikaeen, A., Narayan Babu, H.D., Periyakaruppan, N., and Rfai, T.M.E. (1985), "Structural Bending Properties of High Strength Concrete," ACI *Special Publication* 87-9, American Concrete Institute, Detroit, 147-178.